Clinical Studies

Cancer Research

Favorable Prognostic Impact in Loss of *TP53* and *PIK3CA* Mutations after Neoadjuvant Chemotherapy in Breast Cancer

Yi-Zhou Jiang, Ke-Da Yu, Jing Bao, Wen-Ting Peng, and Zhi-Ming Shao

Abstract

We investigated the loss of somatic mutations in *TP53* and *PIK3CA* in breast cancer tissue after neoadjuvant chemotherapy (NCT) and the clinical relevance of the observed mutation profiles. Samples were derived from three cohorts: Cohort 1 consisting of 206 patients undergoing NCT with matched pre- and postchemotherapy tumor tissues; Cohort 2 consisting of 158 additional patients undergoing NCT; and Cohort 3, consisting of 81 patients undergoing chemotherapy with prechemotherapy tumor tissues. In the first cohort, somatic mutations in *TP53* or *PIK3CA* were identified in 24.8% of the pre-NCT tumor samples but in only 12.1% of the post-NCT tumor samples ($P < 0.001$). Patients with initial *TP53* and *PIK3CA* mutations who became negative for the mutations after NCT had a higher Miller–Payne score ($P = 0.008$), improved disease-free survival, and improved overall survival than those with no change or the opposite change. The association of loss of mutations in *TP53* and *PIK3CA* and improved survival was successfully validated in the second cohort. In addition, 28.4% of the tumors showed intratumoral heterogeneity of somatic mutations in *TP53* or *PIK3CA*, whereas 71.6% were homogeneous, either with or without the mutations. Our data reveal the novel concept that chemotherapy may reduce mutation frequency in patients with breast cancer. Furthermore, the loss of somatic mutations in *TP53* and *PIK3CA* may be translated to biomarkers for prognosis via further verification, which may optimize the choice of sequential therapy and improve patient survival. *Cancer Res; 74(13); 3399–407. ©2014 AACR.*

Introduction

Neoadjuvant chemotherapy (NCT) provides an opportunity to record breast cancer phenotype in a setting where both pre- and postchemotherapy samples can be obtained and the response to chemotherapy can be documented (1). It is of considerable importance to elucidate genetic changes and to identify prognostic biomarkers associated with NCT, which can provide a more accurate assessment of individual treatment. The altered gene expression profiles of breast cancer under NCT have been described (2–4). However, to the best of our knowledge, a comparison of the exomes and genomes of pre- and post-NCT samples does not yet exist. We hypothesized that mutation shift might occur in breast tumors during NCT, and a comparison of the exomes of pre- and post-NCT samples might reveal genetic alterations associated with prognosis.

Recent advances in next-generation sequencing (e.g., whole genome sequencing and exome sequencing) provide further opportunities to more completely characterize the molecular architecture of breast cancer (5, 6). Integrated molecular analyses of breast cancer have revealed that *TP53* and *PIK3CA* are the most frequently mutated genes, each with a mutation frequency >35% (7). Using exome sequencing, we revealed that breast cancers might undergo loss of *TP53* and *PIK3CA* mutations after NCT. This study investigates the loss of *TP53* and *PIK3CA* mutations after NCT and its clinical relevance. This phenomenon, in turn, may serve as prognostic biomarkers and optimize the choice of sequential therapy.

Materials and Methods

Study cohorts

Patients selected for the current study fulfilled the following inclusion criteria: (i) female patients diagnosed with unilateral histologically confirmed invasive ductal carcinoma (IDC); breast carcinoma *in situ* (with or without microinvasion) were excluded; (ii) pathologic examination of tumor specimens was carried out by the Department of Pathology in Fudan University Shanghai Cancer Center (FUSCC, Shanghai, PR China); (iii) patients without any evidence of metastasis at diagnosis. Patients in the first cohort and second cohort had all received three to six cycles of NCT (paclitaxel and carboplatin based)

Authors' Affiliation: Department of Breast Surgery, Fudan University Shanghai Cancer Center; Department of Oncology, Shanghai Medical College, Fudan University, Shanghai, P.R. China

Note: Supplementary data for this article are available at Cancer Research Online (http://cancerres.aacrjournals.org/).

Y.-Z. Jiang, K.-D. Yu, and J. Bao contributed equally to this work.

Corresponding Authors: Zhi-Ming Shao, Department of Breast Surgery, Fudan University Shanghai Cancer Center; Department of Oncology, Shanghai Medical College, Fudan University, 399 Ling-Ling Road, Shanghai, 200032, P.R. China. Phone: 86-15-9219-10483; Fax: 86-21-6443-4556; E-mail: zhimingshao@yahoo.com; and Ke-Da Yu, E-mail: yukd@shca.org.cn

doi: 10.1158/0008-5472.CAN-14-0092

and had residual invasive tumors in the operated breast. In the first cohort, patients were treated at FUSCC between January 1, 2003 and December 31, 2006. In the second cohort for validation of the findings from the first cohort, patients were treated between January 1, 2007 and December 31, 2009. Of the 242 patients who were originally enrolled in the first cohort, 36 patients were considered as pathologic complete remission (pCR) and excluded from the study. Similarly, 30 of the 188 patients initially enrolled in the second cohort were considered pCR and further excluded. As a result, the first cohort consisted of 206 female non-pCR patients with histologically confirmed IDC. The second cohort (the validation cohort) consisted of 158 female non-pCR patients with IDC. Matched samples from biopsies and surgical resection were collected before and after neoadjuvant treatment. Pathologic response was assessed postoperatively using the Miller–Payne scoring system (8, 9), with grade 5 considered to be pCR and grade 1 to 4 to be non-pCR. The third cohort consisted of 81 randomly selected patients with histologically confirmed IDC who had undergone prior surgical resection and received adjuvant chemotherapy. All patients in the third cohort were treated at FUSCC between January 1, 2003 and December 31, 2009.

The molecular subtypes of breast cancer according to immunohistochemical (IHC) profiles were categorized as follows: Luminal A = ER/PR$^+$, HER2$^-$, and Ki67 < 14%; Luminal B = ER/PR$^+$ and HER2$^+$ or Ki67 $\geq$ 14%; HER2$^+$ = ER$^-$, PR$^-$, and HER2$^+$; and basal-like = ER$^-$, PR$^-$, HER2$^-$, and CK5/6$^+$ or EGFR$^+$ (10, 11). Tumors with IHC phenotypes of ER$^-$, PR$^-$, HER2$^-$, CK5/6$^-$, and EGFR$^-$ were excluded. The staining and the interpretation of ER, PR, HER2, Ki-67, CK5/6, and EGFR have been previously described (10, 12). The clinicopathologic characteristics of the patients are listed in Table 1.

Follow-up for patients in the three cohorts was completed on December 31, 2013. The median length of follow-up was 63 months (range, 5–97 months) in the first cohort, 42 months (range, 4–82 months) in the second cohort, and 64 months (range, 5–106 months) in the third cohort. Our definition of disease-free survival (DFS) events included: the first recurrence of disease at a local, regional, or distant site, the diagnosis of contralateral breast cancer, and death from any causes (13). The overall survival (OS) was calculated from the date of diagnosis to the date of death or last follow-up. Patients without events or death were censored at the last follow-up. This study was approved by the Ethics Committee of FUSCC, and each participant signed an informed consent document.

Sample collection and processing

Tumor samples and paired blood samples were obtained from patients undergoing surgical treatment at FUSCC in accordance with the appropriate institutional review boards. For the first and second cohorts, tumor tissues were macrodissected to avoid the influence of stromal tissues (<10%). For each case in the third cohort, one section 15 μm in thickness was stained with hematoxylin and eosin and microdissected using the AS Laser Microdissection system (Leica Microsystems). In total, 30 to 40 tumor foci, each containing approximately 100 cancer cells, were obtained. QIAamp DNA Mini Kits (Qiagen) were used to extract DNA from the tissues. The quality and concentration of the extracted DNA were determined using a NanoDrop 2000 (Thermo Fisher Scientific). The extracted DNA was then used for mutation analysis.

Exome capture and sequencing

DNA extracted from tumor samples and paired blood samples were sent to Beijing Genomics Institute-Shenzhen for exome sequencing as described previously (14–17). Exome capture was done using the SureSelect Human All Exon Kit (Agilent), guided by the manufacturer's protocols. In brief, the qualified genomic DNA samples were randomly fragmented to 200 to 500 bp, followed by end-repair, A-tailing, and paired-end index adapter ligation. Final libraries were validated by Bioanalyzer analysis (Agilent) and quantitative PCR. Each captured library was loaded on the Hiseq 2000 platform and paired-end sequencing was performed with read lengths of 90 bp, providing at least 100-fold average depth for each sample. SOAPaligner 2.20 (18) was used to align the reads to human reference hg19 with parameters set to "-a -b -D -o -v 2 -r 1 -t -n 4." Reads that aligned to the designed target region were collected for single nucleotide variation (SNV) identification and subsequent analysis. For SNV calling, the Variant Quality Score Recalibration method was applied to estimate the probability that each variant is a true genetic variant or a machine artifact. For indel calling, Burrows–Wheeler Aligner (BWA, V.0.5.8) was used to gap align the sequence reads to the human reference hg19. GATK IndelRealigner was used to perform local realignment of the BWA-aligned reads and GATK IndelGentotyperV2 was used to call indels. The variants were functionally annotated and were subsequently categorized into missense, nonsense, read-through, or splice-site mutations and coding indels, which are likely to be deleterious compared with synonymous and noncoding mutations.

Mutation analysis

The detection of mutations in frozen tumor tissues and paired blood DNA was performed by Sanger sequencing of all exons of *TP53* and *PIK3CA*. PCR amplification was performed on an ABI 9700 Thermal Cycler using standard conditions. After amplification, the products were purified using a QIAquick PCR Purification Kit (Qiagen) and directly sequenced using an ABI PRISM 3730 Automated Sequencer (Invitrogen). PCR products were directly sequenced in forward and reverse directions. Detected mutations were confirmed by resequencing of tumor and matched normal blood DNA from new PCR product.

Pyrosequencing, a more sensitive method, was applied to quantitatively re-evaluate the cases with loss of *TP53* or *PIK3CA* mutation after NCT as described previously (19, 20). Allele frequencies were outputted as relative percentages using the Biotage PSQ software.

Statistical analysis

Frequency tabulation and summary statistics were provided to characterize the data distribution. Student *t* test was used to compare continuous variables. To determine the

Table 1. Clinicopathologic characteristics of patients with breast cancer who received neoadjuvant and adjuvant chemotherapy

Characteristics	Cohort 1: NCT ($n = 206$); patient no. (%)	Cohort 2: NCT (n = 158); patient no. (%)	$P1$[a]	Cohort 3: CT ($n = 81$); patient no. (%)	$P2$[b]
Age at diagnosis, y			0.573		0.526
Mean	51	52		53	
SD	9.2	10.1		8.9	
≤50	102 (49.5)	76 (48.1)		36 (44.4)	
>50	104 (50.5)	82 (51.9)		45 (55.6)	
Menopausal status			0.554		0.215
Premenopausal	107 (51.9)	87 (55.1)		37 (45.7)	
Postmenopausal	99 (48.1)	71 (44.9)		44 (54.3)	
(Pre-NCT) Tumor size, cm			0.339		
Mean	4.6	4.9		3.1	<0.001
SD	1.6	1.7		1.2	
<2	41 (19.9)	32 (20.2)		31 (38.3)	
2–5	76 (36.9)	48 (30.4)		37 (45.7)	
>5	89 (43.2)	78 (49.4)		13 (16.0)	
(Pre-NCT) Node status			0.521		0.068
Negative	55 (26.7)	47 (29.7)		31 (38.3)	
Positive	151 (73.3)	111 (70.3)		50 (61.7)	
(Pre-NCT) Tumor grade			0.503		0.221
1–2	60 (29.1)	41 (25.9)		28 (34.6)	
3	146 (70.9)	117 (74.1)		53 (65.4)	
Molecular subtype			0.126		0.601
Luminal A	87 (42.2)	58 (36.7)		38 (46.9)	
Luminal B	49 (23.8)	31 (19.6)		18 (22.2)	
$HER2^+$	24 (11.7)	16 (10.1)		8 (9.9)	
Basal-like	46 (22.3)	53 (33.6)		17 (21.0)	
Pathologic response (Miller–Payne score)			0.041		NA
SD/PD or 1	51 (24.8)	23 (14.6)		NA	
2	49 (23.8)	46 (29.1)			
3	54 (26.2)	55 (34.8)			
4	52 (25.2)	34 (21.5)			
Estimated 3-year DFS			0.732		0.052
Percentage survival	0.768	0.752		0.811	
SE	0.032	0.038		0.048	
Estimated 3-year OS			0.800		0.078
Percentage survival	0.860	0.852		0.901	
SE	0.026	0.031		0.036	

NOTE: All comparisons by χ^2 test except age, tumor size (Student *t* test), and estimated 3-year survival (log-rank test).
Abbreviations: CT, chemotherapy; NA, not applicable.
[a]*P* value between the first and second cohorts.
[b]*P* value between NCT and CT.

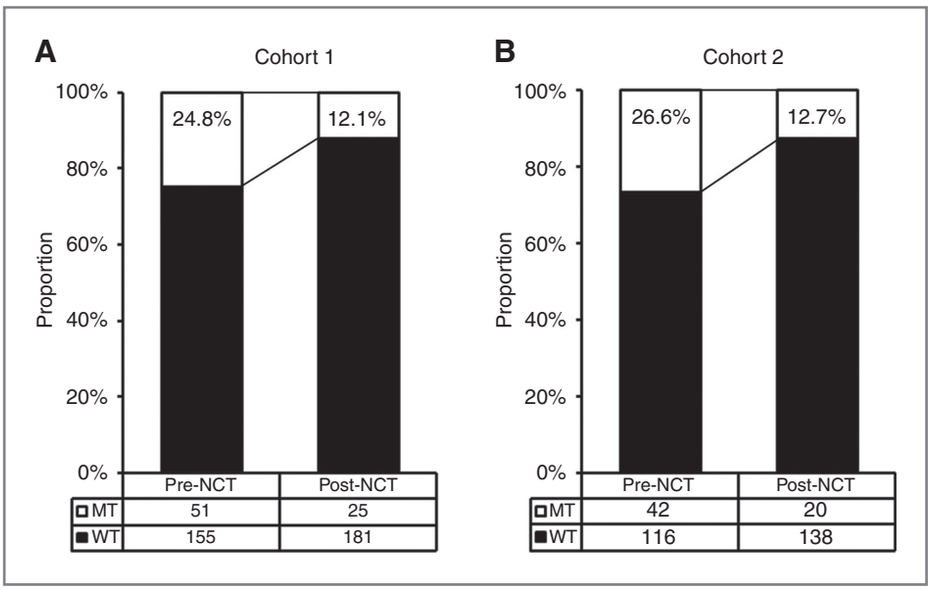

Figure 1. *TP53* and *PIK3CA* mutation shift in tumor tissues before and after NCT in the first (A, $n = 206$) and second cohorts (B, $n = 158$).

combination of *TP53* and *PIK3CA* mutation status, we defined the variable "*TP53* and *PIK3CA* status." The "*TP53* and *PIK3CA* status" was considered wild-type only when neither *TP53* nor *PIK3CA* mutation was detected; otherwise, it was classified as mutant. The McNemar test was applied to compare the change in mutation status following the treatment. The Cochran–Armitage trend test was used to test whether a change in mutation status was associated with clinical outcome in terms of the Miller–Payne Score. Survival curves were constructed using the Kaplan–Meier method, and the univariate survival difference was determined with the log-rank test. Adjusted HRs with 95% confidence intervals (CI) were calculated using Cox proportional hazards models. All statistical analyses were performed using Stata statistical software, version 10.0 (StataCorp). A two-sided $P < 0.05$ was considered statistically significant.

Results

Exome sequencing in two cases for somatic mutation identification

We performed exome sequencing to examine the exomes (100-fold coverage) of two paired samples (pretreatment biopsies and posttreatment tumors), which were separate from the following cohorts. One pair (P1) was from a 62-year-old Chinese woman, and the other (P2) was from a 58-year-old Chinese woman, both of whom were diagnosed with histologically confirmed IDC and received four cycles of NCT (paclitaxel and carboplatin) before undergoing mastectomy (21, 22). Each had an approximately 50% reduction in bidimensionally measurable tumor diameter after NCT. Matched samples from biopsies and surgical resection were collected before and after NCT. Tumors were confirmed as basal-like with IHC phenotypes of ER^-, PR^-, $HER2^-$, $CK5/6^+$, and $EGFR^+$ by two independent pathologists in the Department of Pathology at FUSCC.

By comparing pre- and posttreatment tumor tissues, we identified 23 somatic SNVs in P1 and P2 (Supplementary Table S1). Among these variations, we identified and validated *TP53* (c.C298T) and *PIK3CA* (c.A3140G) as significantly mutated genes only in the pretreatment tumors, not in the paired posttreatment samples, suggesting that *TP53* and *PIK3CA* mutations might be lost in breast cancer after NCT. *TP53* and *PIK3CA* have been identified as the most frequently mutated genes in breast cancer, each with a mutation frequency >35% (7). Thus, we supposed that loss of *TP53* and *PIK3CA* mutations might be a common phenomenon after NCT.

TP53 and *PIK3CA* mutation shift in tumor tissues before and after NCT

We assessed the change in *TP53* and *PIK3CA* mutation status in the first and second cohorts. In pretreatment tumor samples, the frequency of *TP53* mutations was higher in both $HER2^+$ and basal-like breast cancer, and *PIK3CA* mutations were basically associated with Luminal A, Luminal B, and $HER2^+$ status (Supplementary Fig. S1). This was in concordance with the data from the Cancer Genome Atlas (TCGA; ref. 7) and gave confidence to the surrogate molecular subtyping using IHC markers. Both in Cohort 1 and 2, four patients had both *PIK3CA* and *TP53* mutations in the pre-NCT samples, and two patients had both *PIK3CA* and *TP53* mutations in the post-NCT samples. *PIK3CA* and *TP53* mutations are not mutually exclusive in either cohort (Supplementary Table S2, Fisher exact test; in the first cohort, $P = 0.769$ for pre-NCT and $P = 0.217$ for post-NCT; in the second cohort, $P = 0.749$ for pre-NCT and $P = 0.169$ for post-NCT). All *TP53* and *PIK3CA* somatic mutations identified before and after NCT are listed in Supplementary Table S3.

In the first cohort, 51 patients (24.8%) had *TP53* or *PIK3CA* mutations before NCT; this decreased to 25 (12.1%) after treatment (Fig. 1A). Supplementary Figure S2 indicated high viable tumor cellularity in the post-NCT tumors where

Table 2. Association of *TP53* and *PIK3CA* mutation shift with tumor response to NCT in the first cohort ($n = 206$) and second cohort ($n = 158$)

		Miller–Payne Score				
		SD/PD or 1	2	3	4	Total
Cohort	Mutation change	*N* (%)	*N* (%)	*N* (%)	*N* (%)	*N* (%)
First	MT-to-WT	3 (5.9)	5 (10.2)	9 (16.7)	19 (36.5)	36 (17.5)
	WT-to-WT	32 (62.7)	40 (81.6)	42 (77.8)	32 (61.5)	145 (70.4)
	MT-to-MT	10 (19.6)	2 (4.1)	2 (3.7)	1 (1.9)	15 (7.3)
	WT-to-MT	6 (11.8)	2 (4.1)	1 (1.9)	1 (1.9)	10 (4.9)
	Total	51 (100)	49 (100)	54 (100)	52 (100)	206 (100)
Second	MT-to-WT	1 (4.3)	5 (10.9)	9 (16.4)	15 (44.1)	30 (19.0)
	WT-to-WT	10 (43.5)	37 (80.4)	43 (78.2)	18 (52.9)	108 (68.4)
	MT-to-MT	7 (30.4)	2 (4.3)	2 (3.6)	1 (2.9)	12 (7.6)
	WT-to-MT	5 (21.7)	2 (4.3)	1 (1.8)	0 (0)	8 (5.1)
	Total	23 (100)	46 (100)	55 (100)	34 (100)	158 (100)

NOTE: $P < 0.001$ for both the first and second cohorts (Cochran–Armitage trend test).

mutation loss occurred. We also reanalyzed the DNA samples from which mutation loss occurred using pyrosequencing, a more sensitive method, to quantitatively examine the loss of mutations. Compared with pretreatment samples, the post-treatment tumors with loss of *PIK3CA* or *TP53* mutations had significantly decreased frequency (<10%) of mutant alleles (Supplementary Fig. S3). A total of 160 patients (77.7%) retained their initial status [145 wild-type (WT), 15 mutant (MT)]; 10 patients (4.8%) had a WT-to-MT change, and 36 patients (17.5%) had an MT-to-WT change. In the second cohort for validation, 42 patients (26.6%) had *TP53* or *PIK3CA* mutations before NCT; this decreased to 20 (12.7%) after treatment (Fig. 1B). Eight patients (5.1%) had a WT-to-MT change, and 30 patients (19.0%) had an MT-to-WT change; the remaining 120 patients (75.9%) retained their initial status (108 WT, 12 MT). The decrease in mutation rate after chemotherapy was statistically significant in both cohorts ($P < 0.001$; McNemar test for both cohorts). Taken together, these results suggest that loss of *TP53* and *PIK3CA* mutations is common in breast cancer tissues after NCT.

We then evaluated the change in *TP53* and *PIK3CA* mutation status separately (Supplementary Table S4 for the first cohort and Supplementary Table S5 for the second cohort). For *TP53* mutations, the McNemar test revealed that the decrease in the mutation rate after chemotherapy was statistically significant in both cohorts ($P = 0.013$ for the first cohort and $P = 0.035$ for the second cohort). For *PIK3CA* mutations, a similar decrease in the mutation rate was also observed ($P = 0.016$ for the first cohort and $P = 0.019$ for the second cohort). Moreover, molecular subtype was not significantly associated with changes in *TP53* and *PIK3CA* mutations (Supplementary Table S6, $P = 0.902$ for the first cohort and $P = 0.915$ for the second cohort). However, when separately analyzed, $HER2^+$ and basal-like tumors were associated with a higher rate of *TP53* mutation loss (Supplementary Table S7, $P = 0.018$) in the first cohort, but this was not successfully validated in the second cohort (Supplementary Table S7, $P = 0.178$). Molecular subtype was not significantly associated with *PIK3CA* mutation loss (Supplementary Table S8, $P = 0.257$ for the first cohort and $P = 0.404$ for the second cohort).

Influence of mutation shift on tumor response to NCT

We investigated the effect of mutation loss on tumor response to NCT. Patients with Miller–Payne grade 5 (recognized as pCR) were initially excluded from this study because they had no residual cancer tissue after NCT for analysis. Non-pCR patients were divided into four groups: MT-to-WT, WT-to-WT, MT-to-MT, and WT-to-MT. In the first cohort, 106 (51.4%) had significant pathologic partial responses (PR) defined as Miller–Payne grade 3 or 4 (Table 2). In the second cohort, 89 (56.3%) had significant PRs after NCT. Loss of mutation was significantly associated with a better pathologic response ($P < 0.001$ for both the first cohort and second cohort; Cochran–Armitage trend test). In addition, we examined the influence of *TP53* (Supplementary Table S9) or *PIK3CA* (Supplementary Table S10) mutation loss separately on tumor response to NCT. Loss of *TP53* mutation was significantly associated with better clinical response ($P < 0.001$ for the first cohort and $P = 0.001$ for the second cohort; Cochran–Armitage trend test). Loss of *PIK3CA* mutation was also significantly associated with a better pathologic response ($P = 0.001$ for the first cohort and $P < 0.001$ for the second cohort). These data reveal that loss of the *TP53* and *PIK3CA* mutations is associated with improved clinical response to NCT.

Influence of mutation shift on patient survival

We further questioned whether the loss of these mutations influenced DFS and OS. A striking association between loss of mutations in *TP53* and *PIK3CA* and patient survival was observed in both cohorts (Fig. 2). Kaplan–Meier plots showed that mutation change status was associated with DFS ($P = 0.033$) and OS ($P = 0.045$) in the first cohort, and this was likely

Table 3. Multivariate analysis of disease-free survival for patients who underwent NCT in the first cohort ($n = 206$) and second cohort ($n = 158$)

	Cohort 1 ($n = 206$)		Cohort 2 ($n = 158$)	
Variable[a]	**HR (95% CI)**	***P***	**HR (95% CI)**	***P***
TP53 Status				
MT-to-WT	1.00 (Ref.)	0.485	1.00 (Ref.)	0.644
Rest[b]	1.45 (0.91–3.16)		1.17 (0.86–2.73)	
PIK3CA Status				
MT-to-WT	1.00 (Ref.)	0.322	1.00 (Ref.)	0.409
Rest[b]	1.68 (0.59–5.20)		1.57 (0.89–2.59)	
TP53 and *PIK3CA* Status[c]				
MT-to-WT	1.00 (Ref.)	**0.031**	1.00 (Ref.)	**0.042**
Rest[b]	1.96 (1.12–4.88)		1.68 (1.06–3.18)	

NOTE: Bold values indicate statistical significance.

Abbreviation: Ref., reference.

[a]Adjusted by Cox proportional hazards models including age, menopausal status, tumor size, node status, tumor grade, molecular subtype, and pathologic response.

[b]Cases with WT-to-WT, WT-to-MT, or MT-to-MT changes.

[c]To determine the combination of *TP53* and *PIK3CA* mutation status, we defined the variable "*TP53* and *PIK3CA* status." The "*TP53* and *PIK3CA* status" was considered WT only when neither *TP53* nor *PIK3CA* mutation was detected; otherwise, it was classified as MT.

due to the better survival for MT-to-WT group. This observation was supported by similar results from the second cohort ($P = 0.038$ for DFS and $P = 0.058$ for OS). However, neither *TP53* (Supplementary Fig. S4) nor *PIK3CA* (Supplementary Fig. S5) mutation loss alone was significantly associated with DFS, which might be attributable to the limited number of cases with *TP53* or *PIK3CA* mutation loss separately.

Furthermore, we used a multivariate Cox proportional hazards regression model accounting for age, menopausal status, tumor size, lymph node status, grade, molecular

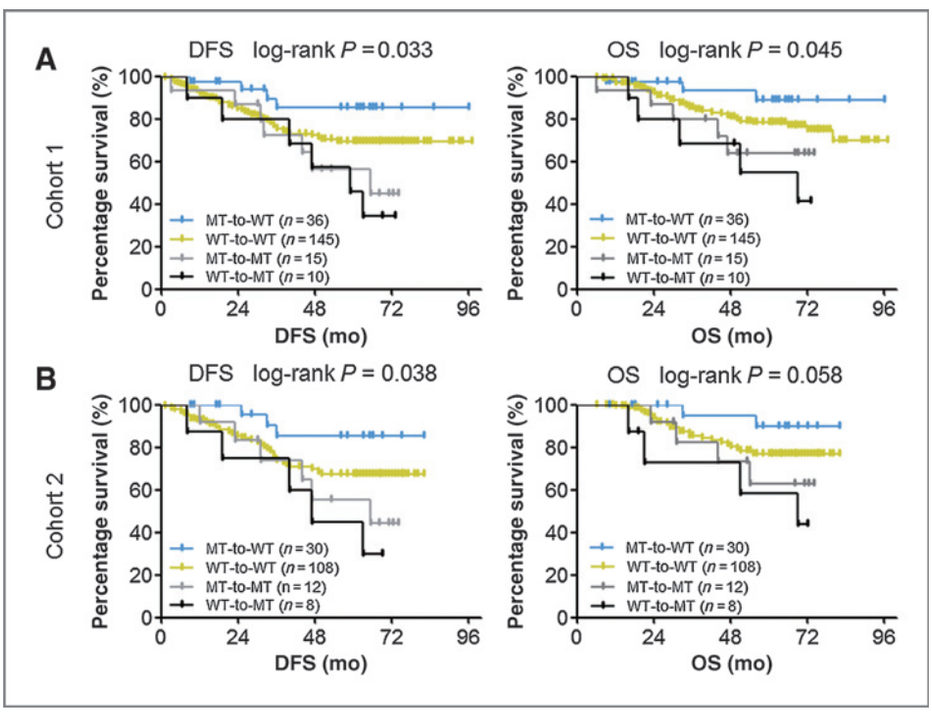

Figure 2. Kaplan–Meier estimates of DFS and OS according to *TP53* and *PIK3CA* mutation shift in the first (A, $n = 206$) and second cohorts (B, $n = 158$).

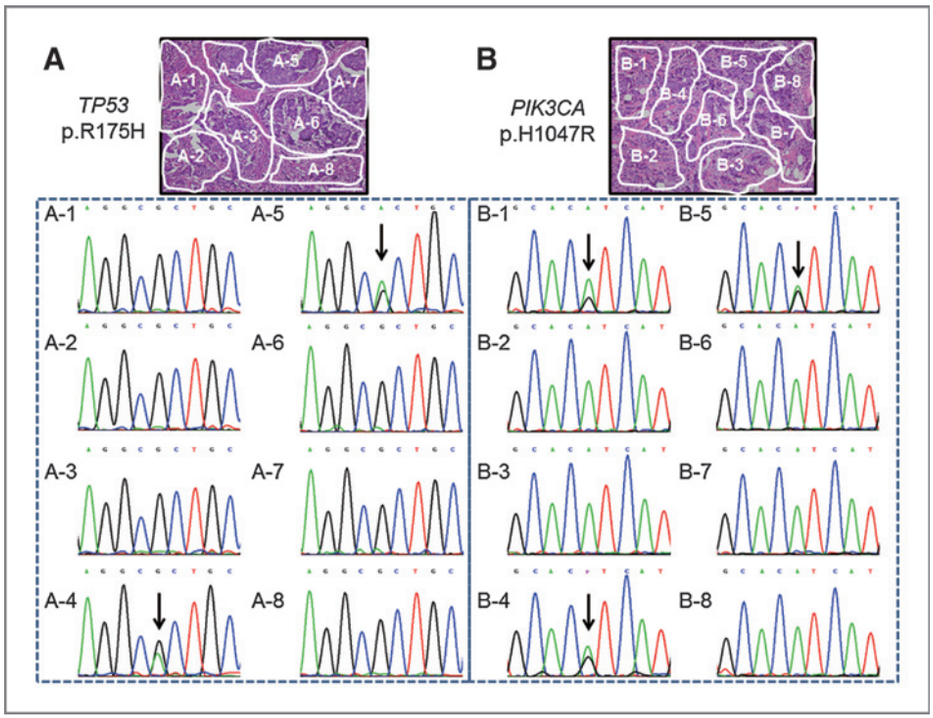

Figure 3. Multiple foci microdissection and analysis of intratumoral heterogeneity of *TP53* and *PIK3CA* somatic mutations in the third cohort ($n = 81$). The arrows indicate somatic mutations. A, representative images of tissue with *TP53* mutation heterogeneity (p.R175H). B, representative images of tissue with *PIK3CA* mutation heterogeneity (p.H1047R). Scale bar, 50 μm.

subtype, pathologic response, and *TP53* and *PIK3CA* status to identify independent predictors of DFS in these two cohorts (Table 3). In the first cohort, we observed that node status, pathologic response, *PIK3CA* status, and *TP53* and *PIK3CA* mutation status were independent predictors of DFS after multivariate adjustment (Supplementary Tables S11 and S12). Compared with the MT-to-WT group, the rest (WT-to-WT, WT-to-MT, and MT-to-MT) were significantly associated with worse DFS (HR, 1.96; 95% CI, 1.12–4.88; $P = 0.031$; Table 3). In the second cohort, the adjusted multivariate regression revealed that tumor size, node status, pathologic response, *PIK3CA* status, and *TP53* and *PIK3CA* mutation status were independent predictors of DFS (Supplementary Tables S11 and S12). The rest (WT-to-WT, WT-to-MT, and MT-to-MT) was also significantly associated with poorer DFS (HR, 1.68; 95% CI, 1.06–3.18; $P = 0.042$; Table 3) relative to an MT-to-WT change. Compared with *TP53* or *PIK3CA* status alone, the combination of *TP53* and *PIK3CA* mutation status was a more robust independent prognostic factor of DFS in both cohorts. Thus, loss of mutations in *TP53* and *PIK3CA* is most likely associated with improved survival.

Intratumoral heterogeneity of mutations in tissue samples

The phenotype of mutation shift prompted us to investigate its biologic nature. We further performed genetic heterogeneity analysis on samples from 81 patients with histologically confirmed IDC who had undergone prior surgical resection and received chemotherapy. Twenty-two cases were *TP53*/*PIK3CA* mutation positive. Of these 22 cases, a total of 748 tumor foci were fractionated. Samples from four of the 22 cases consisted of only MT cells, whereas the other 18 samples consisted of both WT and MT cells. Among the 59 cases identified in routine detection as *TP53* and *PIK3CA* WT by Sanger sequencing, 1,880 tumor foci were fractionated for analysis of *TP53* and *PIK3CA* mutations. Five of the 59 cases consisted of both WT and MT cells. Taken together, 28.4% of the samples (23 of 81) had intratumoral heterogeneity in *TP53* or *PIK3CA* mutation. In Fig. 3, we present typical images of tissues with *TP53* mutation (p.R175H) and *PIK3CA* mutation (p.H1047R) heterogeneity. The remaining 71.6% of the samples (58/81) contained only *TP53*/*PIK3CA* mutation–positive cells or only WT cells. These results reveal high intratumoral heterogeneity of *TP53* and *PIK3CA* in prechemotherapy tumors and partially explain the genetic basis of mutation shift after chemotherapy.

Discussion

To our knowledge, our study is the first to suggest that NCT influences mutation status in tissue samples and to demonstrate that significant loss of mutations in *TP53* and *PIK3CA* can occur during NCT. We highlighted the positive prognostic impact of loss of mutations in *TP53* and *PIK3CA* under NCT in breast cancer. The decreases in the *TP53* and *PIK3CA* mutation rates were significantly associated with better pathologic response (higher Miller–Payne score) and improved survival.

Compared with data released by TCGA (7), our data showed lower mutation rates and different mutation spectra of *TP53* and *PIK3CA* in the pretreatment tumors in Chinese population, indicating that there might be some difference in the mutational evolution of breast cancer in different populations. Since few Asian (or Chinese) patients were included in the TCGA

cohort, it does raise the question of ethnic diversity for future research. As previously reported, the mutation rates and spectra of *TP53* and *PIK3CA* are quite different among different populations. For *PIK3CA* mutations in Chinese population, the mutation rates were 12.3% (7/57) reported by Wang and colleagues (23) and 7.5% (9/120) reported by Tong and colleagues (24). For *TP53* mutations, the frequency of mutation reported by Hao and colleagues (25) was 22.7% (10/44), which was consistent with the results from Fukushima and colleagues (26), who reported 20.0% (10/50) of the tumors harboring *TP53* mutations in the Japanese population. Furthermore, the strength of our study is the reproducibility of the finding in an independent validation sample set. Taken together, our findings, which were in accordance with the previous reports by other Chinese or Asian investigators, revealed unique mutation rates and spectra of *TP53* and *PIK3CA* in Chinese population.

The shift in tumors from mutation status to wild-type status observed in this study suggests that both mutant and nonmutant cancer cells coexist in the same tumor. To identify intratumoral heterogeneity, we microdissected and analyzed mutation status in more than 2,500 tumor foci of 81 tumors from patients with IDC who underwent prior surgery before chemotherapy, and 28.4% of tumors contained both mutant and wild-type foci. These findings are in accordance with the previous reports by Hernandez and colleagues (27) and Kalinsky and colleagues (28).

TP53 and *PIK3CA* are the most commonly mutated genes, and they play pivotal roles in the biology of breast cancer (7). The p53 tumor suppressor protein (encoded by *TP53*) is involved in the cell cycle, checkpoint control, repair of DNA damage, and apoptosis (29–31). *PIK3CA*, encoding the catalytic subunit of phosphoinositide 3-kinase, regulates cell survival, apoptosis, proliferation, motility, growth, and cytoskeletal rearrangement (32–34). Notably, the majority of mutation changes after chemotherapy were from mutant status to wild-type, suggesting that cancer cells harboring certain *TP53* and *PIK3CA* mutations might be more sensitive to chemotherapy than those without mutation. We further analyzed the relationships between the shift of mutation status and tumor response to NCT. We found that patients with a MT-to-WT shift in *TP53* and *PIK3CA* status were more likely to achieve a high Miller–Payne score after chemotherapy; they also had higher DFS rate relative to patients with no change or the opposite change. When considered with previous studies (35, 36), our investigation suggests that mutation shift may be related to the heterogeneity of intratumoral mutations and to different chemosensitivity levels of mutant and wild-type cells. Both mutant and wild-type cancer cells coexist in untreated tumors with *TP53* or *PIK3CA* mutations. For patients who had loss of mutations after NCT, we hypothesize that their cancer cells with certain *TP53* or *PIK3CA* driver mutations might be sensitive to chemotherapeutic agents. Therefore, cytotoxic therapy would primarily remove the mutant cells and consequently shift the evolutionary landscape in favor of the nonmutant subclones. Thus, when analyzing the residual tumors using Sanger sequencing, the percentage of mutant alleles would be too low to detect, and the genotypes of the tumors would be considered to have changed from MT to WT. These patients generally had smaller residual tumors, benefited more from adjuvant chemotherapy and had relatively favorable prognosis. In contrast, for patients who underwent MT-to-MT change or WT-to-MT change after NCT, their cancer cells with *TP53* or *PIK3CA* driver mutations might be resistant to chemotherapeutic agents. In the residual tumors, the mutant alleles would remain or become enriched. Consequently, these patients benefited less from chemotherapy and had relatively poor prognosis. Interestingly, in the third cohort, five patients (6.2%) had a low frequency and abundance of *TP53*/*PIK3CA* mutations, which were detected only through microsamples, thus explaining in part why the mutation status of some patients shifted from negative to positive after chemotherapy.

One of the limitations of the current study is the lack of sufficient pre-NCT tumor tissue for microdissection and mutation analysis. We therefore used the third cohort for the analysis of intratumoral heterogeneity of *TP53* and *PIK3CA* mutations, and the results from the three interconnecting cohorts provide a solid foundation to support our conclusions. In addition, more research is required to elucidate the mechanism by which loss of mutations in *TP53* and *PIK3CA* regulates chemosensitivity. The regimen used in these patients was a combination of taxanes and platinum. In fact, both taxanes (mitotic inhibitors and antimicrotubule agents) and platinum (DNA-damaging agents) might be relevant for the mutation loss. However, the precise mechanism of mutation loss is beyond the current study. Further studies are warranted to explore molecular mechanisms resulting in the chemotherapy-related loss of mutations in *TP53* and *PIK3CA*.

In conclusion, chemotherapy may affect somatic mutation status in patients with breast cancer, lowering the number of *TP53* and *PIK3CA* mutations. This may be attributable to the heterogeneity of intratumoral mutations and the different sensitivities of mutant and wild-type tumor cells to chemotherapy. These findings might help to optimize the choice of sequential therapy and improve patient survival. To enable the selection of the most effective therapeutic option, additional preclinical and clinical studies based on our findings are needed to further examine drug resistance mechanisms and to validate our findings in other independent cohorts.

Disclosure of Potential Conflicts of Interest

No potential conflicts of interest were disclosed.

Authors' Contributions

Conception and design: Y.-Z. Jiang, K.-D. Yu, J. Bao, Z.-M. Shao
Development of methodology: Y.-Z. Jiang, K.-D. Yu
Acquisition of data (provided animals, acquired and managed patients, provided facilities, etc.): Y.-Z. Jiang, J. Bao, W.-T. Peng
Analysis and interpretation of data (e.g., statistical analysis, biostatistics, computational analysis): Y.-Z. Jiang, K.-D. Yu, J. Bao, W.-T. Peng
Writing, review, and/or revision of the manuscript: Y.-Z. Jiang, K.-D. Yu, J. Bao, W.-T. Peng, Z.-M. Shao
Administrative, technical, or material support (i.e., reporting or organizing data, constructing databases): K.-D. Yu, Z.-M. Shao
Study supervision: K.-D. Yu, Z.-M. Shao

Acknowledgments

The authors thank Jiong Wu, Jin-Song Lu, Guang-Yu Liu, Gen-Hong Di, and Zhen-Zhou Shen for excellent data handling.

Grant Support

This work was supported by National Natural Science Foundation of China (81370075, 81001169), Training Plan of Excellent Talents in Shanghai Municipality Health System (K.-D. Yu), Research and Innovation Project of Shanghai Municipal Education Commission (2014; K.-D. Yu), Shanghai International Science and Technique Cooperation Foundation (12410707700), International S&T Cooperation Program of China (ISTCP No. 09), and the Shanghai Key Laboratory of Breast Cancer (12DZ2260100).

The costs of publication of this article were defrayed in part by the payment of page charges. This article must therefore be hereby marked *advertisement* in accordance with 18 U.S.C. Section 1734 solely to indicate this fact.

Received January 14, 2014; revised April 14, 2014; accepted April 15, 2014; published OnlineFirst June 12, 2014.

References

1. Ellis MJ, Ding L, Shen D, Luo J, Suman VJ, Wallis JW, et al. Whole-genome analysis informs breast cancer response to aromatase inhibition. Nature 2012;486:353–60.
2. Modlich O, Prisack HB, Munnes M, Audretsch W, Bojar H. Immediate gene expression changes after the first course of neoadjuvant chemotherapy in patients with primary breast cancer disease. Clin Cancer Res 2004;10:6418–31.
3. Buchholz TA, Stivers DN, Stec J, Ayers M, Clark E, Bolt A, et al. Global gene expression changes during neoadjuvant chemotherapy for human breast cancer. Cancer J 2002;8:461–8.
4. Lee SC, Xu X, Lim YW, Iau P, Sukri N, Lim SE, et al. Chemotherapy-induced tumor gene expression changes in human breast cancers. Pharmacogenet Genomics 2009;19:181–92.
5. Shah SP, Roth A, Goya R, Oloumi A, Ha G, Zhao Y, et al. The clonal and mutational evolution spectrum of primary triple-negative breast cancers. Nature 2012;486:395–9.
6. Stephens PJ, Tarpey PS, Davies H, Van Loo P, Greenman C, Wedge DC, et al. The landscape of cancer genes and mutational processes in breast cancer. Nature 2012;486:400–4.
7. Cancer Genome Atlas Network. Comprehensive molecular portraits of human breast tumours. Nature 2012;490:61–70.
8. Ogston KN, Miller ID, Payne S, Hutcheon AW, Sarkar TK, Smith I, et al. A new histological grading system to assess response of breast cancers to primary chemotherapy: prognostic significance and survival. Breast 2003;12:320–7.
9. Silver DP, Richardson AL, Eklund AC, Wang ZC, Szallasi Z, Li Q, et al. Efficacy of neoadjuvant Cisplatin in triple-negative breast cancer. J Clin Oncol 2010;28:1145–53.
10. Kennecke H, Yerushalmi R, Woods R, Cheang MC, Voduc D, Speers CH, et al. Metastatic behavior of breast cancer subtypes. J Clin Oncol 2010;28:3271–7.
11. Voduc KD, Cheang MC, Tyldesley S, Gelmon K, Nielsen TO, Kennecke H. Breast cancer subtypes and the risk of local and regional relapse. J Clin Oncol 2010;28:1684–91.
12. Goldhirsch A, Wood WC, Coates AS, Gelber RD, Thurlimann B, Senn HJ. Strategies for subtypes–dealing with the diversity of breast cancer: highlights of the St. Gallen international expert consensus on the primary therapy of early breast cancer 2011. Ann Oncol 2011;22:1736–47.
13. Yu KD, Huang AJ, Fan L, Li WF, Shao ZM. Genetic variants in oxidative stress-related genes predict chemoresistance in primary breast cancer: a prospective observational study and validation. Cancer Res 2012;72:408–19.
14. Yan XJ, Xu J, Gu ZH, Pan CM, Lu G, Shen Y, et al. Exome sequencing identifies somatic mutations of DNA methyltransferase gene DNMT3A in acute monocytic leukemia. Nat Genet 2011;43:309–15.
15. Li Y, Vinckenbosch N, Tian G, Huerta-Sanchez E, Jiang T, Jiang H, et al. Resequencing of 200 human exomes identifies an excess of low-frequency non-synonymous coding variants. Nat Genet 2010;42:969–72.
16. Zang ZJ, Cutcutache I, Poon SL, Zhang SL, McPherson JR, Tao J, et al. Exome sequencing of gastric adenocarcinoma identifies recurrent somatic mutations in cell adhesion and chromatin remodeling genes. Nat Genet 2012;44:570–4.
17. Jiang YZ, Yu KD, Peng WT, Di GH, Wu J, Liu GY, et al. Enriched variations in TEKT4 and breast cancer resistance to paclitaxel. Nat Commun 2014;5:3802.
18. Li R, Yu C, Li Y, Lam TW, Yiu SM, Kristiansen K, et al. SOAP2: an improved ultrafast tool for short read alignment. Bioinformatics 2009;25:1966–7.
19. Lai LA, Kostadinov R, Barrett MT, Peiffer DA, Pokholok D, Odze R, et al. Deletion at fragile sites is a common and early event in Barrett's esophagus. Mol Cancer Res 2010;8:1084–94.
20. Amos-Landgraf JM, Kwong LN, Kendziorski CM, Reichelderfer M, Torrealba J, Weichert J, et al. A target-selected Apc-mutant rat kindred enhances the modeling of familial human colon cancer. Proc Natl Acad Sci U S A 2007;104:4036–41.
21. Chen XS, Nie XQ, Chen CM, Wu JY, Wu J, Lu JS, et al. Weekly paclitaxel plus carboplatin is an effective nonanthracycline-containing regimen as neoadjuvant chemotherapy for breast cancer. Ann Oncol 2010;21:961–7.
22. Yu KD, Liu GY, Zhou XY, Zhou Y, Wu J, Chen CM, et al. Association of HER-2 copy number and HER-2/CEP-17 ratio with neoadjuvant taxane-containing chemotherapy sensitivity in locally advanced breast cancer. Oncologist 2012;17:792–800.
23. Wang L, Zhang Q, Zhang J, Sun S, Guo H, Jia Z, et al. PI3K pathway activation results in low efficacy of both trastuzumab and lapatinib. BMC Cancer 2011;11:248.
24. Tong L, Yang XX, Liu MF, Yao GY, Dong JY, Ye CS, et al. Mutational analysis of key EGFR pathway genes in Chinese breast cancer patients. Asian Pac J Cancer Prev 2012;13:5599–603.
25. Hao XD, Yang Y, Song X, Zhao XK, Wang LD, He JD, et al. Correlation of telomere length shortening with TP53 somatic mutations, polymorphisms and allelic loss in breast tumors and esophageal cancer. Oncol Rep 2013;29:226–36.
26. Fukushima T, Onda M, Abe R, Otake T, Kimijima I, Tsuchiya A. p53 mutations and overexpressions in Japanese breast cancer. Eur J Surg Oncol 1995;21:595–600.
27. Hernandez L, Wilkerson PM, Lambros MB, Campion-Flora A, Rodrigues DN, Gauthier A, et al. Genomic and mutational profiling of ductal carcinomas in situ and matched adjacent invasive breast cancers reveals intra-tumour genetic heterogeneity and clonal selection. J Pathol 2012;227:42–52.
28. Kalinsky K, Heguy A, Bhanot UK, Patil S, Moynahan ME. PIK3CA mutations rarely demonstrate genotypic intratumoral heterogeneity and are selected for in breast cancer progression. Breast Cancer Res Treat 2011;129:635–43.
29. Kastan MB, Bartek J. Cell-cycle checkpoints and cancer. Nature 2004;432:316–23.
30. Brosh R, Rotter V. When mutants gain new powers: news from the mutant p53 field. Nat Rev Cancer 2009;9:701–13.
31. Lehmann BD, Pietenpol JA. Targeting mutant p53 in human tumors. J Clin Oncol 2012;30:3648–50.
32. Barbareschi M, Buttitta F, Felicioni L, Cotrupi S, Barassi F, Del GM, et al. Different prognostic roles of mutations in the helical and kinase domains of the PIK3CA gene in breast carcinomas. Clin Cancer Res 2007;13:6064–9.
33. Shaw RJ, Cantley LC. Ras, PI(3)K and mTOR signalling controls tumour cell growth. Nature 2006;441:424–30.
34. Bader AG, Kang S, Zhao L, Vogt PK. Oncogenic PI3K deregulates transcription and translation. Nat Rev Cancer 2005;5:921–9.
35. Bai H, Wang Z, Chen K, Zhao J, Lee JJ, Wang S, et al. Influence of chemotherapy on EGFR mutation status among patients with non-small-cell lung cancer. J Clin Oncol 2012;30:3077–83.
36. Mok TS, Wu YL, Thongprasert S, Yang CH, Chu DT, Saijo N, et al. Gefitinib or carboplatin-paclitaxel in pulmonary adenocarcinoma. N Engl J Med 2009;361:947–57.